Network Parameters for
"*Uncovering Load-Altering Attacks Against N 1 Secure Power Grids: A Rare-Event Sampling Approach*"

Maldon Patrice Goodridge [a], Subhash Lakshminarayaya[b] and Alessandro Zocca[c]

[a]Global Development Initiatives, UK
[b]School of Engineering, University of Warwick, Coventry, UK
[c]Department of Mathematics, Vrije Universiteit Amsterdam, NL

July 16, 2023

## Contents



# 1 Automatic Voltage Regulation

This section is reproduced from the supplementary information for [1], from which the power system model is derived.

The AVR scheme we use in the present work is summarized in Figure 1. Using as input value the voltage of the generic bus $i$, through a series of transformations, this protocol determines a voltage affecting the Rotor's field $E_{f,i}$. The AVR comprises of a Sensor, which measures the voltage through a potential transformer, an Amplifier, which magnifies the deviation w.r.t. a reference value, and an Exciter, which finally produces the potential impacting the generator.

In the engineering literature [2], this sequence of transformations is usually expressed by means of transfer functions which describe the effect of each device in terms of its input/output Laplace transform. To avoid proliferation of notation, we indicate the Laplace transform of an observable by changing its argument label, for instance $E_i(z) = \mathcal{L}[E_i(t)](z)$ [1]. In this way, having in mind the components in Figure 1, the Sensor, Amplifier, and Exciter are defined as

$$\frac{\nu_i^s(z)}{E_i(z)} := \frac{K_i^s}{1+zT_i^s}, \quad \frac{\epsilon_i^a(z)}{z^{-1}V_i^r - \nu_i^s(z)} := \frac{K_i^a}{1+zT_i^a}, \quad \text{and} \quad \frac{\nu(z)}{\epsilon_i^a(z)} := \frac{K_i^e}{1+zT_i^e}, \tag{1}$$

[1]As a quick reference for the Reader, we define the Laplace transform as $\mathcal{L}[f(t)](z) := \int_{-\infty}^{\infty} f(t)e^{-zt}dt$ where $z$ is a complex variable and $f(t)$ a time-varying function.

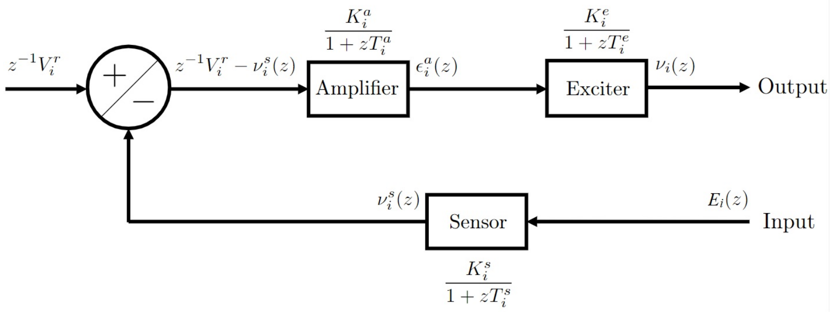


Figure 1: Diagram of the AVR scheme. The input voltage $E_i(t)$ is Laplace transformed and is then multiplied for the Sensor transfer function. The circle takes the difference between $E_i^s(t)$ and the reference value $V^r$ (the $z^{-1}$ prefactor is equal to 1 when inverse Laplace transformed, see (2b)). The result is used as the input of the Amplifier. The output value of the Exciter can be brought back to the time domain via the inverse Laplace transform. In the main text, we follow a different approach in which we inverse Laplace transform the action of each component of the diagram. The resulting input/output process is summarized in (2).

respectively, where the $K_i > 0$ are dimensionless quantities and the $T_i > 0$ are time constants. By bringing all the terms to the numerator, e.g. for the Sensor $\nu_i^s(z) + T_i^s z \nu_i^s(z) = K_i^s \nu_i(z)$, and then taking the inverse Laplace transform[2], we obtain the AVR scheme described in terms of a system of first-order differential equations

$$\begin{cases} \dot{\nu}_i^s(t) = \dfrac{1}{T_i^s}\big(K_i^s \nu_i(t) - \nu_i^s(t)\big) & \text{(2a)} \\ \dot{\epsilon}_i^a(t) = \dfrac{1}{T_i^a}\Big(K_i^a\big(V_i^r - \nu_i^s(t)\big) - \epsilon_i^a(t)\Big). & \text{(2b)} \\ \dot{\nu}_i(t) = \dfrac{1}{T_i^e}\big(K_i^e \epsilon_i^a(t) - \nu(t)\big) & \text{(2c)} \end{cases}$$

In practice, as the numerical solution of the power grid differential equation involves time discretisation, the output value of $\nu_i$ at time $t$ is used for the evaluation of the voltage at the next time step, which generates a new $E_i$ to be fed in the AVR.

[2]The inverse Laplace transform is defined as $\mathcal{L}^{-1}[f(z)](t) := \frac{1}{2\pi i} \lim_{T\to\infty} \int_{\gamma-iT}^{\gamma+iT} f(z)e^{zt}dz$. The usual assumptions hold that is the integration is done along the vertical line $\gamma$ chosen to be greater than the real part of all singularities of $f(z)$ which is assumed to be bounded on this line.

# 2 Network Variable Parameters

This section details the parameter values implemented during the study.

## 2.1 IEEE 39 Network

| **Sym.** | **Description** | Scenario | **Values** | **U** |
|---|---|---|---|---|
| $\delta^0$ | Electrical Phase Angle (nodal; t = 0) | Night | [ 0.9827 ,0.9879 ,0.9992 , 1.0072, 1.0039, 1.0143, 1.0236, 1.0044, 1.0238, 0.9529, 0.9578 0.9400, 0.9423, 0.9682, 0.9631 0.9690, 0.9849, 0.9779, 0.9941, 0.9694, 0.9780, 0.9724 0.9643, 0.9858, 0.9966, 0.9608, 0.9617 ] | [ |
| | | Morning | [0.9107, 0.9389, 0.9974, 1.0366, 1.0194, 1.0734, 1.1210, 1.0214, 1.1215, 0.7598, 0.7843, 0.6936, 0.7052, 0.8375, 0.8111, 0.8413, 0.9226, 0.8866, 0.9695, 0.8431, 0.8867, 0.8583, 0.8171 0.9264, 0.9818, 0.7994, 0.8042] | [ |
| | | Afternoon | [ 0.9294, 0.9513, 0.9975, 1.0291, 1.0156, 1.0581, 1.0959, 1.0173, 1.0965, 0.8094, 0.8289, 0.7569, 0.7661, 0.8711, 0.8502, 0.8743, 0.9387, 0.9102, 0.9759, 0.8757, 0.9103, 0.8877, 0.8550, 0.9419, 0.9859, 0.8409, 0.8447] | [ |
| | | Evening | [ 0.6598, 0.6965, 0.7519, 0.8355, 0.8282, 0.8862, 0.9860, 0.8393, 1.0002, 0.3871, 0.4451, 0.3008, 0.3185, 0.5225, 0.4898, 0.5383, 0.6710, 0.6060, 0.7371, 0.5409, 0.6213, 0.5787, 0.5105, 0.6928, 0.7808, 0.4767, 0.4843] | [ |
| $\dot{\delta}^0$ | Rotor Angular Velocity (nodal; t = 0) | - | $[0, 0, \ldots, 0, 0] \in \mathbb{R}^{27} \forall \tau$ | [ |
| $\ddot{\delta}^0$ | Rate of Change of Frequency (nodal; t= 0) | - | $[0, 0, \ldots, 0, 0, ] \in \mathbb{R}^{27} \forall \tau$ | [ |
| $E^0$ | Voltages (nodal; t= 0) | Night | [ 0.9582, 0.9753, 0.9914, 0.9927, 0.9907, 0.9785, 1.0066, 0.9832, 0.9720, 0.9877, 0.9862, 0.9722, 0.9765, 0.9787, 0.9773, 0.9797, 0.9744, 0.9770, 0.9826, 0.9755, 0.9817, 0.9752, 0.9704 0.9722, 0.9784, 0.9754, 0.9715] | [ |
| | | Morning | [0.9531, 0.9657, 0.9793, 0.9829, 0.9834, 0.9672, 0.9959, 0.9751, 0.9601, 0.9830, 0.9762, 0.9655, 0.9685, 0.9718, 0.9697, 0.9710, 0.9655, 0.9665, 0.9698, 0.9670, 0.9736, 0.9685, 0.9650 0.9642, 0.9668, 0.9688, 0.9659] | [ |
| | | Afternoon | [0.9550, 0.9694, 0.9840, 0.9867, 0.9862, 0.9715, 1.0000, 0.9782, 0.9647, 0.9848, 0.9800, 0.9681, 0.9716, 0.9745, 0.9726, 0.9743, 0.9689, 0.9705, 0.9747, 0.9703, 0.9767, 0.9711, 0.9671 0.9672, 0.9712, 0.9714, 0.9680] | [ |
| | | Evening | [0.9558, 0.9534, 0.9653, 0.9698, 0.9722, 0.9523, 0.9790, 0.9629, 0.9591, 0.9760, 0.9629, 0.9563, 0.9576, 0.9633, 0.9596, 0.9592, 0.9526, 0.9522, 0.9511, 0.9553, 0.9624, 0.9597, 0.9578 0.9556, 0.9562, 0.9602, 0.9584] | [ |
| $\chi^{G,0}$ | Generator Power (nodal; t= 0) | Night | [ 1.00, 1.908, 2.60, 2.528, 2.032, 2.60, 2.24, 2.16, 3.32, 4.00, 0, 0, . . . , 0, 0] | p |
| | | Morning | [2.5, 4.771, 6.5, 6.32, 5.08, 6.5, 5.6, 5.4, 8.3, 10.0, 0, 0, . . . , 0, 0] | [ |
| | | Afternoon | [2.125, 4.0553, 5.525, 5.372, 4.318, 5.525, 4.76, 4.59, 7.055, 8.5, 0, 0, . . . , 0, 0] | [ |
| | | Evening | [3.25, 6.2023, 8.45, 8.216, 6.604, 8.45, 7.28, 7.02, 10.79, 13.0, 0, 0 . . . , 0, 0] | [ |
| $\chi^{L,0}$ | Loads (nodal; t= 0) | Night | [0, 0.0368, 0, 0, 0, 0, 0, 0, 0, 4.4160, 2.0000, 0.9352, 2.0880, 0.0300, 1.2800, 1.3160, 2.5120, 1.0960, 0.9900, 1.2344, 0.8960, 0.5560, 1.124, 0.8240, 1.1340, 1.2880, 0.6320] | [ |
| | | Morning | [0, 0.0920, 0, 0, 0, 0, 0, 0, 0, 11.0400, 5.0000, 2.3380, 5.2200, 0.0750, 3.2000, 3.2900, 6.2800, 2.7400, 2.4750, 3.0860, 2.2400, 1.3900, 2.810, 2.0600, 2.8350, 3.2200, 1.5800] | [ |
| | | Afternoon | [0, 0.0782, 0, 0, 0, 0, 0, 0, 0, 9.3840, 4.2500, 1.9873, 4.4370, 0.0638, 2.7200, 2.7965, 5.3380, 2.3290, 2.1038, 2.6231, 1.9040, 1.1815, 2.3885 1.7510, 2.4097, 2.7370, 1.3430 ] | [ |
| | | Evening | [0, 0.1196, 0, 0, 0, 0, 0, 0, 0, 14.3520, 6.5000, 3.0394, 6.7860, 0.0975, 4.1600, 4.2770, 8.1640, 3.5620, 3.2175, 4.0118, 2.9120, 1.8070, 3.6530, 2.6780, 3.6855, 4.1860, 2.0540 ] | [ |
| $D$ | Load Damping Factor | - | 2 | [ |
| $S$ | Transient Time constant (commonly denoted $T'_{d0}$) | - | [7.0000, 6.5600 , 5.7000 , 5.6900, 5.4000 , 7.3000 , 5.6600, 6.7000 , 4.7900 , 10.2000 ] | [ |
| $E_{f,i}$ | Rotor Field Voltage | - | 0.95 | [ |
| | | | **Governor Parameters** | |
| $A$ | Governor Droop Response | - | 2 | M |
| $\mathcal{W}$ | Governor Dead-band Frequency Range | - | $[59.95, 60.05]$ | [ |
| | | | **AVR Parameters** | |
| $T^s$ | Sensor Time Constant | - | 0.05 | [ |
| $K^s$ | Sensor Gain Constant | - | 1 | |
| $T^a$ | Amplifier Time Constant | - | 0.1 | [ |
| $K^a$ | Amplifier Gain Constant | - | 10 | |
| $T^e$ | Exciter Time Constant | - | 1 | [ |
| $K_e$ | Exciter Gain Constant | - | 10 | |
| | | | **Protection Systems Parameters** | |
| $F^+$ | OFGS Threshold | - | 62 | [ |
| $T^{of}$ | OFGS Relay Delay | - | 2 | [ |
| $G^+, G^-$ | RoCoF Trip Threshold | - | -3, 3 | [ |
| $T^{ro}$ | RoCoF Relay Delay | - | 1 | [ |
| $F^-$ | UFLS Threshold | - | $\{59.5, 59, 58.5, 58, 57.5\}$ | [ |
| $T^{uf}$ | UFLS Relay Delay | - | 2 | [ |
| $P^\phi$ | Line Trip Power Flow Deviation Threshold | - | 510 | [ |
| $T^\phi$ | Line Trip Relay Delay | - | 4 | [ |
| | | | **Two Area Generator Data** | |
| $P^{max}$ | Maximum Generator Power | - | [900, 900, 900, 900, 900, 900, 1000, 1000, 1500, 1500] | [ |
| $H$ | Generator Inertia Constants | - | [5, 3.03, 3.58, 2.86, 4.33, 3.48, 2.64, 2.43, 3.45, 4.2] | [ |
| $X_d'$ | Transient Reactance | - | 4.05 | [ |
| $X_d$ | Sub-transient reactance | - | 2.93 | [ |
| $B$ | line susceptances | - | see below | [ |

Table of parameters used in simulations conducted on the Two-Area Network.

$$
B = \begin{bmatrix}
-42.1988 & 0 & 0 & 0 & 0 & 0 & 0 & 0 & 0 & 3.7656 & 0 & 0 & 0 \\
0 & -35.5333 & 2.1965 & 0 & 0 & 0 & 0 & 0 & 0 & 0 & 20.6982 & 0 & 7.4273 \\
0 & 2.1965 & -37.4811 & 0 & 0 & 0 & 0 & 0 & 0 & 0 & 16.4849 & 0 & 3.6444 \\
0 & 0 & 0 & -45.8275 & 0 & 0 & 0 & 0 & 0 & 0 & 0 & 0 & 0 \\
0 & 0 & 0 & 0 & -55.417 & 0 & 0 & 0 & 0 & 0 & 0 & 0 & 0 \\
0 & 0 & 0 & 0 & 0 & -50.6771 & 0 & 0 & 0 & 0 & 0 & 0 & 0 \\
0 & 0 & 0 & 0 & 0 & 0 & -36.7523 & 0 & 0 & 0 & 0 & 0 & 0 \\
0 & 0 & 0 & 0 & 0 & 0 & 0 & -43.0746 & 0 & 0 & 0 & 0 & 0 \\
0 & 0 & 0 & 0 & 0 & 0 & 0 & 0 & -63.9344 & 0 & 0 & 0 & 0 \\
3.7656 & 0 & 0 & 0 & 0 & 0 & 0 & 0 & 0 & -28.7041 & 0 & 0 & 16.4592 \\
0 & 20.6982 & 16.4849 & 0 & 0 & 0 & 0 & 0 & 0 & 0 & -168.9438 & 0 & 46.8403 \\
0 & 0 & 0 & 0 & 0 & 0 & 0 & 0 & 0 & 0 & 0 & -215.7208 & 215.7598 \\
0 & 7.4273 & 3.6444 & 0 & 0 & 0 & 0 & 0 & 0 & 16.4592 & 46.8403 & 215.7598 & -293.7623 \\
0 & 2.3492 & 8.7981 & 0 & 0 & 0 & 0 & 0 & 0 & 0 & 17.6005 & 0 & 3.8895 \\
0 & 0.7184 & 4.1052 & 0 & 0 & 0 & 0 & 0 & 0 & 0 & 23.632 & 0 & 1.1832 \\
0 & 0 & 0 & 18.9558 & 0 & 0 & 0 & 0 & 0 & 0 & 0 & 0 & 0 \\
0 & 0 & 0 & 25.3661 & 54.9227 & 0 & 0 & 0 & 0 & 0 & 0 & 0 & 0 \\
0 & 0 & 0 & 0 & 0 & 20.1418 & 0 & 0 & 0 & 0 & 0 & 0 & 0 \\
0 & 0 & 0 & 0 & 0 & 29.3615 & 36.7523 & 0 & 0 & 0 & 0 & 0 & 0 \\
0 & 0 & 0 & 0 & 0 & 0 & 0 & 0 & 0 & 0 & 0 & 0 & 0 \\
21.2592 & 0 & 0 & 0 & 0 & 0 & 0 & 42.024 & 0 & 5.8459 & 0 & 0 & 0 \\
0 & 0 & 0 & 0 & 0 & 0 & 0 & 0 & 0 & 0 & 0 & 0 & 0 \\
0 & 0 & 0 & 0 & 0 & 0 & 0 & 0 & 0 & 0 & 0 & 0 & 0 \\
0 & 0 & 0 & 0 & 0 & 0 & 0 & 0 & 0 & 0 & 0 & 0 & 0 \\
0 & 0 & 0 & 0 & 0 & 0 & 0 & 0 & 62.375 & 0 & 0 & 0 & 0 \\
16.3457 & 0 & 0 & 0 & 0 & 0 & 0 & 0 & 0 & 4.6879 & 46.7741 & 0 & 0 \\
0 & 0 & 0 & 0 & 0 & 0 & 0 & 0 & 0 & 0 & 0 & 0 & 0
\end{bmatrix}
$$

$$
\left.\begin{array}{ccccccccccccc}
\dots & 0 & 0 & 0 & 0 & 0 & 21.2592 & 0 & 0 & 0 & 16.34 & 57 & 0 \\
\dots & 0 & 0 & 0 & 0 & 0 & 0 & 0 & 0 & 0 & 0 & 0 & 0 \\
\dots & 0 & 0 & 0 & 0 & 0 & 0 & 0 & 0 & 0 & 0 & 0 & 0 \\
\dots & 18.9558 & 25.3661 & 0 & 0 & 0 & 0 & 0 & 0 & 0 & 0 & 0 & 0 \\
\dots & 0 & 54.9227 & 0 & 0 & 0 & 0 & 0 & 0 & 0 & 0 & 0 & 0 \\
\dots & 0 & 0 & 20.1418 & 29.3615 & 0 & 0 & 0 & 0 & 0 & 0 & 0 & 0 \\
\dots & 0 & 0 & 0 & 36.7523 & 0 & 0 & 0 & 0 & 0 & 0 & 0 & 0 \\
\dots & 0 & 0 & 0 & 0 & 0 & 42.024 & 0 & 0 & 0 & 0 & 0 & 0 \\
\dots & 0 & 0 & 0 & 0 & 0 & 0 & 0 & 0 & 0 & 62.375 & 0 & 0 \\
\dots & 0 & 0 & 0 & 0 & 0 & 5.8459 & 0 & 0 & 0 & 0 & 4.6879 & 0 \\
\dots & 0 & 0 & 0 & 0 & 0 & 0 & 0 & 0 & 0 & 0 & 46.7741 & 0 \\
\dots & 0 & 0 & 0 & 0 & 0 & 0 & 0 & 0 & 0 & 0 & 0 & 0 \\
\dots & 0 & 0 & 0 & 0 & 0 & 0 & 0 & 0 & 0 & 0 & 0 & 0 \\
\dots & 0 & 0 & 0 & 0 & 0 & 0 & 0 & 0 & 0 & 0 & 0 & 0 \\
\dots & 105.4166 & 0 & 0 & 0 & 0 & 0 & 0 & 0 & 0 & 0 & 0 & 0 \\
\dots & -452.7209 & 19.6858 & 73.8149 & 0 & 169.0544 & 0 & 0 & 22.1387 & 0 & 0 & 0 & 46.6323 \\
\dots & 19.6858 & -100.3665 & 0 & 0 & 0 & 0 & 0 & 0 & 0 & 0 & 0 & 0 \\
\dots & 73.8149 & 0 & -123.7523 & 30.6077 & 0 & 0 & 0 & 0 & 0 & 0 & 0 & 0 \\
\dots & 0 & 0 & 30.6077 & -124.0966 & 28.459 & 0 & 0 & 0 & 0 & 0 & 0 & 0 \\
\dots & 169.0544 & 0 & 0 & 28.459 & -197.2989 & 0 & 0 & 0 & 0 & 0 & 0 & 0 \\
\dots & 0 & 0 & 0 & 0 & 0 & -122.6283 & 30.6588 & 0 & 0 & 0 & 25.0386 & 0 \\
\dots & 0 & 0 & 0 & 0 & 0 & 30.6588 & -133.5865 & 67.4157 & 20.9248 & 15.868 & 0 & 0 \\
\dots & 22.1387 & 0 & 0 & 0 & 0 & 0 & 67.4157 & -113.2189 & 0 & 0 & 0 & 24.0033 \\
\dots & 0 & 0 & 0 & 0 & 0 & 0 & 20.9248 & 0 & -86.071 & 65.6607 & 0 & 0 \\
\dots & 0 & 0 & 0 & 0 & 0 & 0 & 15.868 & 0 & 65.6607 & -141.7435 & 0 & 0 \\
\dots & 0 & 0 & 0 & 0 & 0 & 25.0386 & 0 & 0 & 0 & 0 & -166.5271 & 74.6771 \\
\dots & 46.6323 & 0 & 0 & 0 & 0 & 0 & 0 & 24.0033 & 0 & 0 & 74.6771 & -145.0171
\end{array}\right]
$$

| **Generator** | Rating **(MVA)** | $X_d$ **(pu)** | $X_d^{'}$ **(pu)** | $T_{d0}^{'}$ **(s)** | $H$ **(s)** |
|---|---|---|---|---|---|
| G1 | 900 | 0.1 | 0.031 | 10.2 | 500 |
| G2 | 900 | 0.295 | 0.0697 | 6.56 | 30.3 |
| G3 | 900 | 0.2495 | 0.0531 | 5.7 | 35.8 |
| G4 | 900 | 0.262 | 0.0436 | 5.69 | 28.6 |
| G5 | 900 | 0.67 | 0.132 | 5.4 | 26 |
| G6 | 900 | 0.254 | 0.05 | 7.3 | 34.8 |
| G7 | 1000 | 0.295 | 0.049 | 5.66 | 26.4 |
| G8 | 1000 | 0.29 | 0.057 | 6.7 | 24.3 |
| G9 | 1500 | 0.2106 | 0.057 | 4.79 | 34.5 |
| G10 | 1500 | 0.02 | 0.006 | 7 | 500 |

Table 2: Generator Data for the IEEE 39 network, Four Node Network: 1000 MVA base

| From Bus | To Bus | R (pu) | X (pu) | B (pu) |
|---|---|---|---|---|
| 1 | 2 | 0.0035 | 0.0411 | 0.6987 |
| 1 | 39 | 0.001 | 0.025 | 0.75 |
| 2 | 3 | 0.0013 | 0.0151 | 0.2572 |
| 2 | 25 | 0.007 | 0.0086 | 0.146 |
| 3 | 4 | 0.0013 | 0.0213 | 0.2214 |
| 3 | 18 | 0.0011 | 0.0133 | 0.2138 |
| 4 | 5 | 0.0008 | 0.0128 | 0.1342 |
| 4 | 14 | 0.0008 | 0.0129 | 0.1382 |
| 5 | 6 | 0.0002 | 0.0026 | 0.0434 |
| 5 | 8 | 0.0008 | 0.0112 | 0.1476 |
| 6 | 7 | 0.0006 | 0.0092 | 0.113 |
| 6 | 11 | 0.0007 | 0.0082 | 0.1389 |
| 7 | 8 | 0.0004 | 0.0046 | 0.078 |
| 8 | 9 | 0.0023 | 0.0363 | 0.3804 |
| 9 | 39 | 0.001 | 0.025 | 1.2 |
| 10 | 11 | 0.0004 | 0.0043 | 0.0729 |
| 10 | 13 | 0.0004 | 0.0043 | 0.0729 |
| 13 | 14 | 0.0009 | 0.0101 | 0.1723 |
| 14 | 15 | 0.0018 | 0.0217 | 0.366 |
| 15 | 16 | 0.0009 | 0.0094 | 0.171 |
| 16 | 17 | 0.0007 | 0.0089 | 0.1342 |
| 16 | 19 | 0.0016 | 0.0195 | 0.304 |
| 16 | 21 | 0.0008 | 0.0135 | 0.2548 |
| 16 | 24 | 0.0003 | 0.0059 | 0.068 |
| 17 | 18 | 0.0007 | 0.0082 | 0.1319 |
| 17 | 27 | 0.0013 | 0.0173 | 0.3216 |
| 21 | 22 | 0.0008 | 0.014 | 0.2565 |
| 22 | 23 | 0.0006 | 0.0096 | 0.1846 |
| 23 | 24 | 0.0022 | 0.035 | 0.361 |
| 25 | 26 | 0.0032 | 0.0323 | 0.513 |
| 26 | 27 | 0.0014 | 0.0147 | 0.2396 |
| 26 | 28 | 0.0043 | 0.0474 | 0.7802 |
| 26 | 29 | 0.0057 | 0.0625 | 1.029 |
| 28 | 29 | 0.0014 | 0.0151 | 0.249 |
| 12 | 11 | 0.0016 | 0.0435 | 0 |
| 12 | 13 | 0.0016 | 0.0435 | 0 |
| 6 | 31 | 0 | 0.025 | 0 |
| 10 | 32 | 0 | 0.02 | 0 |
| 19 | 33 | 0.0007 | 0.0142 | 0 |
| 20 | 34 | 0.0009 | 0.018 | 0 |
| 22 | 35 | 0 | 0.0143 | 0 |
| 23 | 36 | 0.0005 | 0.0272 | 0 |
| 25 | 37 | 0.0006 | 0.0232 | 0 |
| 2 | 30 | 0 | 0.0181 | 0 |
| 29 | 38 | 0.0008 | 0.0156 | 0 |
| 19 | 20 | 0.0007 | 0.0138 | 0 |

Table 2: Transmission Network Data for the IEEE 39 Test Network: 100 MVA, 60 Hz base. [3]

# 3 KTAS Parameters

The following susceptance matrices describe the reduce KTAS network before and after the line tripping. As explained in Section 2(a) of the main text, the susceptance matrix depends on the indicator function $\Omega$ which flips from 1 to 0 when a line tripping occurs. The difference occurs in line 5-6, which is the inter-connector line of the partially reduced network. So in the stationary regime we have

$$B(1) = \begin{bmatrix} -18.9278 & 7.8461 & 0 & 0 & 12.9499 & 0 \\ 7.8461 & -38.0413 & 0 & 0 & 32.5581 & 0 \\ 0 & 0 & -19.0178 & 7.8461 & 0 & 12.9499 \\ 0 & 0 & 7.8461 & -38.3713 & 0 & 32.5581 \\ 12.9499 & 32.5581 & 0 & 0 & -52.1891 & 9.0982 \\ 0 & 0 & 12.9499 & 32.5581 & 9.0982 & -50.6891 \end{bmatrix},$$

and after the line tripping

$$B(0) = \begin{bmatrix} -18.9278 & 7.8461 & 0 & 0 & 12.9499 & 0 \\ 7.8461 & -38.0413 & 0 & 0 & 32.5581 & 0 \\ 0 & 0 & -19.0178 & 7.8461 & 0 & 12.9499 \\ 0 & 0 & 7.8461 & -38.3713 & 0 & 32.5581 \\ 12.9499 & 32.5581 & 0 & 0 & -52.1891 & 0 \\ 0 & 0 & 12.9499 & 32.5581 & 0 & -50.6891 \end{bmatrix}.$$

| **Sym.** | **Description** | Scenario | **Meaning** | **Units** |
|---|---|---|---|---|
| $\delta^0$ | Electrical Phase Angle (nodal; t = 0) | Night | $[0.125, 0.0853, 0.0069, -0.0162, 0.0415, -0.0341]$ | |
| | | Morning | [ 0.3672 , 0.189 , -0.0885 , -0.2666 , -0.0664 , -0.5216 ] | |
| | | Afternoon | [ 0.1635 , 0.0943 , 0.0085 , -0.0653 , -0.0213 , -0.1415 ] | |
| | | Evening | [ 0.3519 , 0.1627 , -0.0797 , -0.2338 , -0.115 , -0.5204 ] | [rad] |
| $\dot{\delta}^0$ | Rotor Angular Velocity (nodal; t = 0) | - | $[0, 0, 0, 0, 0, 0]$ | $[s^{-1}]$ |
| $\ddot{\delta}^0$ | Rate of Change of Frequency (nodal; t= 0) | - | $[0, 0, 0, 0, 0, 0, ]$ | $[s^{-2}]$ |
| $E^0$ | Voltages (nodal; t= 0) | - | 230 | kV |
| $\chi^{G,0}$ | Generator Power (nodal; t= 0) | Night | [ 100 , 100 , 100 , 100 , 0 , 0 ] | |
| | | Morning | [ 783.5 , 783.5 , 733.5 , 733.5 , 0 , 0 ] | |
| | | Afternoon | [ 400 , 450 , 370 , 330 , 0 , 0 ] | |
| | | Evening | [ 870 , 880 , 870 , 900 , 0 , 0 ] | $[MW]$ |
| $\chi^{L,0}$ | Loads (nodal; t= 0) | Night | [ 10 , 10 , 10 , 10 , 180 , 180 ] | |
| | | Morning | [ 100 , 100 , 50 , 50 , 967 , 1767 ] | |
| | | Afternoon | [ 150 , 150 , 100 , 100 , 500 , 550 ] | |
| | | Evening | [ 150 , 150 , 200 , 100 , 1100 , 1820 ] | $[MW]$ |
| $D$ | Load Damping Factor | - | 2 | [%] |
| $S$ | Transient Time constant | - | 8 | [s] |
| $E_{f,i}$ | Rotor Field Voltage | - | 20 | [kV] |
| | **Governor Parameters** | | | |
| $A$ | Governor Droop Response | - | 2 | MW/$\Delta f$ |
| $\mathcal{W}$ | Governor Dead-band Frequency Range | - | $[59.95, 60.05]$ | [Hz] |
| | **Protection Systems Parameters** | | | |
| $F^+$ | OFGS Threshold | - | 62 | [Hz] |
| $T^{of}$ | OFGS Relay Delay | - | 2 | [s] |
| $G^+, G^-$ | RoCoF Trip Threshold | - | -3, 3 | $[Hzs^{-2}]$ |
| $T^{ro}$ | RoCoF Relay Delay | - | 1 | [s] |
| $F^-$ | UFLS Threshold | - | $\{59.5, 59, 58.5, 58, 57.5\}$ | [Hz] |
| $T^{uf}$ | UFLS Relay Delay | - | 2 | [s] |
| $P^{\phi}$ | Line Trip Power Flow Deviation Threshold | - | 510 | [MW] |
| $T^{\phi}$ | Line Trip Relay Delay | - | 4 | [s] |
| | **Two Area Generator Data** | | | |
| $P^{max}$ | Maximum Generator Power | - | 900 | [MW] |
| $H$ | Generator Inertia Constant | - | 6.5, 6.175 | [s] |
| $X_d$ | Transient Reactance | - | 4.05 | [ohms] |
| $X_d^{'}$ | Sub-transient reactance | - | 2.93 | [ohms] |
| $B$ | line susceptances | - | see below | [siemens] |

Table 1: Table of parameters used in simulations conducted on the Two-Area Network.

| **Generator** | Rating **(MVA)** | $X_d$ **(pu)** | $X_d^{'}$ **(pu)** | $T_{d0}^{'}$ **(s)** | $H$ **(s)** |
|---|---|---|---|---|---|
| G1 | 900 | 1.8 | 0.3 | 8 | 6.5 |
| G1 | 900 | 1.8 | 0.3 | 8 | 6.5 |
| G1 | 900 | 1.8 | 0.3 | 8 | 6.175 |
| G1 | 900 | 1.8 | 0.3 | 8 | 6.175 |

Table 3: Generator Data for the Two-Area, Four Node Network: 900 MVA, 20kV base

| **From Bus** | **To Bus** | **R (pu)** | **X (pu)** | **B (pu)** |
|---|---|---|---|---|
| 1 | 5 | 0 | 0.15/9 | 0 |
| 2 | 6 | 0 | 0.15/9 | 0 |
| 3 | 11 | 0 | 0.15/9 | 0 |
| 4 | 10 | 0 | 0.15/9 | 0 |
| 5 | 6 | 25×0.0001 | 25×0.001 | 25×0.00175 |
| 10 | 11 | 25×0.0001 | 25×0.001 | 25×0.00175 |
| 6 | 7 | 10×0.0001 | 10×0.001 | 10×0.00175 |
| 9 | 10 | 10×0.0001 | 10×0.001 | 10×0.00175 |
| 7 | 8 | 110×0.0001 | 110×0.001 | 110×0.00175 |
| 7 | 8 | 110×0.0001 | 110×0.001 | 110×0.00175 |
| 8 | 9 | 110×0.0001 | 110×0.001 | 110×0.00175 |
| 8 | 9 | 110×0.0001 | 110×0.001 | 110×0.00175 |

Table 2: Transmission Network Data for the Two-Area, Four Node Network: 100 MVA, 230kV base. [4]

# References


[1] Maldon Patrice Goodridge, John Moriarty, and Andrea Pizzoferrato. A rare-event study of frequency regulation and contingency services from grid-scale batteries. *Philos. Trans. Royal Soc. A*, 379(2202):20190433, 2021.

[2] K Eswaramma and G Surya Kalyan. An Automatic Voltage Regulator (AVR) system control using a P-I-DD controller. *International Journal of Advance Engineering and Research Development*, 4(6), 2017.

[3] M.A. Pai. *Energy Function Analysis for Power System Stability.* Power Electronics and Power Systems. Springer US, 2012.

[4] Prabha Kundur, Neal J Balu, and Mark G Lauby. *Power system stability and control*, volume 7. McGraw-hill New York, 1994.